Very high gain single pass two–beam coupling in 'blue' $Rh:BaTiO_3$

M. Kaczmarek * R. W. Eason

Optoelectronics Research Centre and Department of Physics
University of Southampton, Southampton S017 1BJ, U.K.
fax: +44 1703 593142, tel: +44 1703 593144
e-mail: mfk@orc.soton.ac.uk

Abstract

Two–beam coupling has been studied at red and near–infrared wavelengths in 'blue' $Rh:BaTiO_3$. High amplification, of the order of 20 000 – 37 000, of a weak signal beam, has been measured. $Rh:BaTiO_3$ exhibits strong intensity–dependent absorption and transmission behaviour and this effect is considered when fitting theoretical plots to the experimental data.

*On leave from the Department of Physics, A. Mickiewicz University, 60-780 Poznań, Poland.

$BaTiO_3$ is one of the best known and most efficient photorefractive materials. Its ability to couple light efficiently has been widely utilised to observe numerous nonlinear processes. The recent upsurge of interest in materials with strong infrared response stimulated research in improving the near-infrared sensitivity of these crystals. As a result, a new type of $BaTiO_3$ was grown, blue in colour, with rhodium as a main dopant [1, 2]. This Rh:$BaTiO_3$ proved to have significantly increased red and infrared absorption and also high reflectivities of self-pumped phase conjugation across this spectrum of wavelengths [3]. Our earlier studies of the optical properties of Rh:$BaTiO_3$ showed strong intensity-dependent effects, namely light-induced transparency. The changes in absorption have been successfully modelled numerically assuming additional secondary photorefractive centres [4].

Here we describe the recent progress in exploring the capability of Rh:$BaTiO_3$ to amplify very weak signals. Utilising its high sensitivity at red and infrared wavelengths we have investigated the two-beam coupling process at several different wavelengths and observed significantly large gains. We have measured gains, as high as 22 000, generated over only 3 mm thick crystal, and 37 000 obtained from a 7 mm thick crystal. To our knowledge this is the highest beam coupling gain reported so far.

In the past, nominally undoped $BaTiO_3$ was often used for image and weak signal amplification. High values of gain, of the order of several thousand, were achieved [5, 6, 7] due to the large electro-optic coefficients of $BaTiO_3$. However, at the optimum configuration for two beam coupling strong beam fanning is also present. The two processes compete and as a result, the amplified signal to noise ratio is low, and the magnitude of gain is significantly reduced. Attempts to obtain beam coupling gain as high as predicted by the standard two-beam coupling theory involved experimental schemes aimed at reducing the process of fanning. In this way large values of gain ($\sim$ 11 000) were obtained utilising the observed difference in build-up times of two-beam coupling and fanning gratings [7]. Alternatively, beam fanning from the strong pump beam was employed in a multi-pass coupling arrangement with a signal beam. This experiment, involving 'light crawling', showed an enhancement of gain in thin samples of $LiNbO_3$ [8]. In our experimental configuration of two-beam coupling in Rh:$BaTiO_3$, fanning effects appear to have minimal destructive influence on the gain observed.

The two-beam coupling gain was measured experimentally as the ratio of the signal beam intensity (I_s) in the presence of a coherent pump beam (I_p) to the signal beam intensity in the absence of a coherent pump beam, conventionally expressed as:

$$G = \frac{I_s \; with \; I_p \; present}{I_s \; with \; I_p \; absent} \tag{1}$$

Assuming the undepleted pump approximation, and plane wave interaction, the relation (1) can be expressed as:

$$G = \frac{(1+\beta_o)\exp(\Gamma L)}{1+\beta_o \; \exp(\Gamma L)} \tag{2}$$

which is the well–known standard theory relation between the magnitude of the two–beam coupling gain, G, and the incident intensity ratio, $\beta_o = I_s/I_p$. Γ is the coupling coefficient, which can be calculated from the material parameters and the experimental configuration, and L is the interaction length. Using expression (2), the theoretical value of gain G can be computed.

In order to investigate the beam coupling efficiency of $Rh{:}BaTiO_3$ we used three different wavelengths: 647 nm, 800 nm and 1.06 μm. $Rh{:}BaTiO_3$ exhibits very strong absorption in the red (4.2 cm^{-1} at 650 nm) and hence, at first, we decided to optimise the beam coupling process at 647 nm to obtain the maximum gain in a simple experimental configuration. The sample of $Rh{:}BaTiO_3$ (7 mm × 3 mm × 5.6 mm) was illuminated by a 3 mm diameter pump beam, and a 1 mm diameter signal beam originating from a Kr^+ laser. The beam crossing angle and the position of the crystal was chosen to optimise the coupling coefficient Γ. The external angles of incidence were 64.5^o for the pump beam and 12^o for the signal beam. The angle between the grating vector and the crystal's c axis was 13.5^o. We measured beam coupling in two configurations, first along the 3 mm face of the crystal, and then along the 7 mm face. In both cases the interaction lengths were limited by the crystal length.

Figure 1 presents a typical gain dependence on the input power ratio for the case when both beams propagated along the 3 mm side of the crystal. The very high magnitude of gain   22 000   indicates a coupling coefficient of 33.8 cm^{-1} (standard fit) and 32.6 cm^{-1} (corrected model). These values agree well with the theoretical prediction of 32.9 cm^{-1}, calculated from the material equations and using the value of unclamped electro–optic coefficients for $BaTiO_3$.

Figure 2 shows the beam coupling gain obtained when both beams propagated along the 7 mm face of the crystal. As before, an extremely high value of gain – 37 000 – was observed. On both figures the standard theory curve, based on equation (2), is plotted as a dashed line with Γ as a fitting parameter. The values of coupling coefficient Γ obtained from the theoretical fits (15.8 and 16.5 cm^{-1}) are in this case much smaller than the magnitude calculated from the material equations (32.9 cm^{-1}). This discrepancy is typical for two–beam coupling in the presence of strong fanning. From this result and the very good agreement between the values of Γ determined experimentally and calculated theoretically in the case of short interaction length, it can be concluded that the 3 mm interaction length provides optimum (or close to optimum) conditions for beam coupling without the destructive influence of fanning.

From comparing experimental data with theoretical curves it can be seen that the standard theory does not provide a very good fit to the experimental data. However, this difference is not surprising as the effect of light-induced transparency, indicating the presence of secondary photorefractive centres, is quite strong. Strong intensity–dependent absorption means that the absorption coefficient experienced by the signal beam depends on whether the strong pump beam is present or not. In the simplest way, this effect introduces a correction to the expression for the beam coupling gain in a form of an additional term $\exp(\Delta\alpha L)$. As a result, a better theoretical fit to experimental data can be found (solid lines in Figures 1 and 2), especially for the case of the longer interaction length (Figure 2). To obtain these curves, Γ was used as a fitting parameter, while the change in the absorption coefficient $\Delta\alpha$ has been determined from an independent experiment. The corrected theoretical curves still do not fit the data perfectly well, but reproduce quite reliably the general trend of gain dependence on the beam ratio observed experimentally. Figure 3 presents light-induced transparency observed at 647 nm. The maximum measured change in the absorption coefficient reached 0.9 cm^{-1}, and this value was used as a fixed parameter in our theoretical fitting procedure.

An interesting feature, which is worth noting, is that the gain didn't saturate for the range of beam ratios we used in the experiments, either for 3 mm or 7 mm interaction lengths. To observe saturation of beam coupling, which occurs here for extremely small beam ratios, would require a more extended experimental set-up involving a very good laser stabilisation and amplifiers. The theoretical curves (Figure 1) predict a saturated value of gain of approximately 24 000 – 25 000 (3 mm interaction length), which is close to the experimentally observed magnitude of 22 000. Theoretical gain curves presented in Figure 2 saturate at values as high as 100 000 – 120 000, which leaves an interesting possibility for future experiments in long samples of Rh:$BaTiO_3$.

To investigate the build-up of the grating between the signal and pump beam, we monitored the temporal behaviour of the amplified signal beam. Three traces presented in Figure 4 show its time evolution. The intensity of the signal beam slowly increases with time, until reaching an approximately constant value. Further, small variations of this value originate, most probably, from some competition with beam fanning. The differences between traces, especially in the first several seconds, arise from the different, immediate previous exposure of the crystal before the measurement. However, the final, steady–state value of signal intensity is reliably repeatable. Generally, the more thoroughly all residual gratings were erased before each measurement, the longer it took the signal beam to reach the maximum value. Trace 1 is the best example of this effect. Shorter illumination (trace 2) or no pre–illumination (trace 3) between measurements helped a faster development of a strong, amplified signal.

Different temporal development of amplified signals can be regarded as an indication of a general tendency of Rh:$BaTiO_3$ to depend strongly on its history. Rh:$BaTiO_3$ appears to be quite sensitive to pre–illumination with light and its initial response can vary significantly. Depending on the temperature and storage conditions the temporal behaviour of absorption and beam coupling can therefore be quite different. Fortunately, the response stabilises after a few hours of laser illumination. This effect is currently under further quantitative study in our laboratory.

Following the studies of beam coupling at the wavelength of maximum absorption for Rh:$BaTiO_3$, we investigated its response at the near–infrared. Finite absorption at 800 nm ($\alpha = 1.5\,cm^{-1}$) allowed us to observe energy exchange between the beams, however, the maximum gain measured was only approximately 150, obtained using the 3 mm interaction length geometry. The magnitude of coupling coefficient which can be deduced from this gain, namely 17 cm^{-1}, is much smaller than that for 647 nm, but it is nevertheless significant for beam coupling at infrared wavelengths in $BaTiO_3$. Using Ti:Sapphire laser illumination, we investigated beam coupling with other wavelengths from the near-infrared regime (730–810 nm) and obtained values of gain similar to the 800 nm case.

In order to investigate the extreme end of operation of $Rh:BaTiO_3$ we set-up the two-beam coupling with 1.06 μm CW radiation from a Nd:YAG laser. Despite the negligibly small value for absorption at this wavelength ($\alpha = 0.06\ cm^{-1}$) we were still able to observe a finite gain of approximately 21 (with the 3 mm interaction length). This is equivalent to a coupling coefficient of 11 cm^{-1}. Figure 5 presents the experimental data of gain at 1.06 μm, together with the standard theory curve for different input beam ratios (dashed line). Additionally, as before, we plotted the theoretical curve with correction for intensity-dependent absorption. As can be seen in Figure 5, in this case the corrected curve does not improve the fit. It is important to add that at 1.06 μm we observed light-induced absorption, in contrast to light-induced transparency at 647 nm. This increased absorption possibly aided the beam coupling efficiency. To determine the maximum increase of absorption with intensity we performed a separate experiment and measured this change to be approximately equal to 0.4 cm^{-1}. This value was then used in theoretical fitting. The detailed analysis and modelling of intensity and wavelength dependent absorption will be discussed in a separate work.

It should be noted that the gains observed in all the experiments were achieved without any need for suppressing beam fanning. The beam coupling in the configuration we used proved much stronger than interaction with scattered light, which is responsible for light fanning.

In conclusion, we have presented extremely efficient two-beam coupling results at 647 nm in $Rh:BaTiO_3$ with a record high magnitude of gain. The significant values of gain observed at near-infrared wavelengths indicate a promising application of these crystals to work with cheap laser sources at 800 nm, such as laser diodes. The simple theoretical fitting procedure we used does not fit the experimental data absolutely satisfactory, but it is just the first attempt to reproduce the experimental results. Possibly numerical simulation of full two-beam coupling theory with different photorefractive centres can provide a better model. We further aim to investigate the response of $Rh:BaTiO_3$ to pre-sensitisation with light, as it may hold a key to a further improvement of its response.

We would like to thank Mark Garrett from Deltronic Crystal Industries and Daniel Rytz for supplying us with Rh:$BaTiO_3$ and their collaboration in the work on characterisation of these crystals. We also gratefully acknowledge the contribution to this work from Petr Hribek from the Technical University in Prague and Graeme Ross from ETH in Zürich. We thank the Laser Division, Rutherford Appleton Laboratory, Chilton, Didcot, UK, for the Ti:Sapphire laser used in this research.

References

[1] C. Warde, T. W. McNamara, M. H. Garrett, P. Tayebati, SPIE Conference, San Diego, CA, CR48-07, July 1993.

[2] B. A. Wechsler, M. B. Klein, C. C. Nelson, R. N. Schwartz, Opt. Lett. **19**, 536 (1994).

[3] G. W. Ross, P. Hribek, R. W. Eason, M. H. Garrett, D. Rytz, Opt. Commun. **101**, 60 (1993).

[4] M. Kaczmarek, G. W. Ross, P. M. Jeffrey, R. W. Eason, P. Hribek, M. J. Damzen, R. Ramos–Garcia, R. Troth, M. H. Garrett, D. Rytz, Optical Materials, **4**, 158 (1995).

[5] Y. Fainman, E. Klancnik, S.H. Lee, Opt. Eng. **25**, 228 (1986).

[6] F. Laeri, T. Tschudi, J. Albers, Opt. Commun. **47**, 387 (1983).

[7] J. Joseph, P.K.C. Pillai, K. Singh, Appl. Opt. **30** , 3315 (1991).

[8] J. Zhang, W. Sun, H. Zhao, S. Bian, K. Xu, M. Li, Y. Xu, Opt. Lett. **18**, 1391 (1993).

Figure captions

Figure 1 Two-beam coupling at 647 nm with 3 mm interaction length.
Circles: experimental data, dashed line: standard theory fit $\Gamma = 33.8\ cm^{-1}$, sold line: standard theory fit with correction for change in absorption coefficient $\Delta\alpha = 0.9\ cm^{-1}$, $\Gamma = 32.6\ cm^{-1}$.

Figure 2 Two–beam coupling at 647 nm with 7 mm interaction length.
Circles: experimental data, dashed line: standard theory fit $\Gamma = 16.5\ cm^{-1}$, solid line: standard theory fit with correction for change in absorption coefficient $\Delta\alpha = 0.9\ cm^{-1}$, $\Gamma = 15.8\ cm^{-1}$.

Figure 3 Intensity–dependent absorption coefficient at 647 nm.
Solid line is plotted to help to visualise experimental points using two–level saturable absorber model ($\alpha = \alpha_1 + \alpha_0/(1 + I/I_{sat})$, where $\alpha_1 = 4.82$, $\alpha_0 = 0.86$, $I_{sat} = 11.8\ mW/cm^2$).

Figure 4 Temporal evolution of the two–beam coupling signal.
The measurements of three traces were separated by several minutes and different light exposure before measurements: trace 1: long pre–illumination with light, trace 2: short pre–illumination with light trace 3: no pre–illumination with light.

Figure 5 Two–beam coupling gain at 1.06 μm.
Circles: experimental data, dashed line: standard theory curve with $\Gamma = 11\ cm^{-1}$, solid line: standard theory fit with correction for change in absorption coefficient $\Delta\alpha = -0.4\ cm^{-1}$, $\Gamma = 11.2\ cm^{-1}$, $L = 0.3\ cm$.

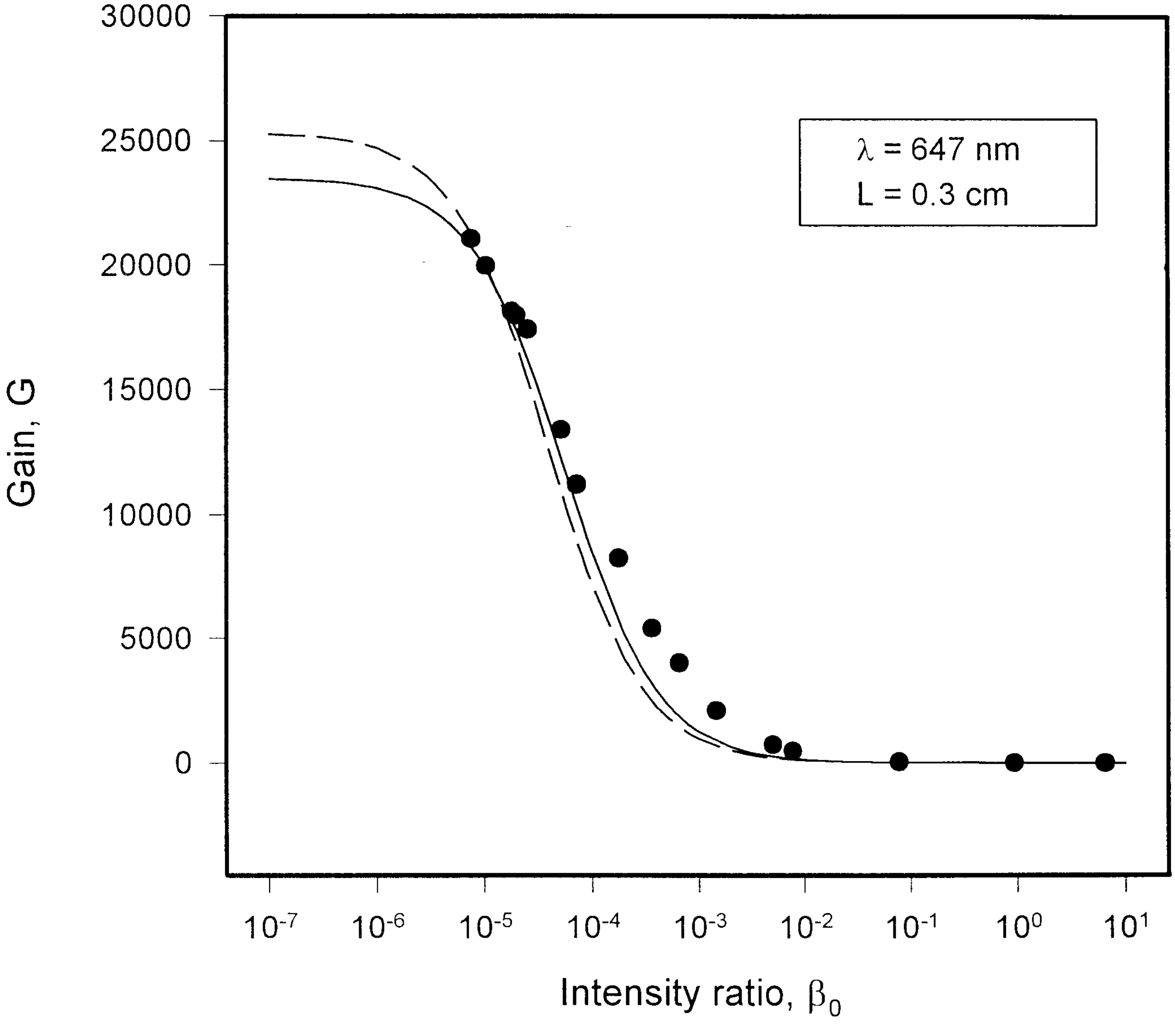

30000
25000
20000
15000
10000
5000
0
Gain, G
λ = 647 nm
L = 0.3 cm
10-7
10-6
10-5
10-4
10-3
10-2
10-1
100
101
Intensity ratio, β0

Fig. 1

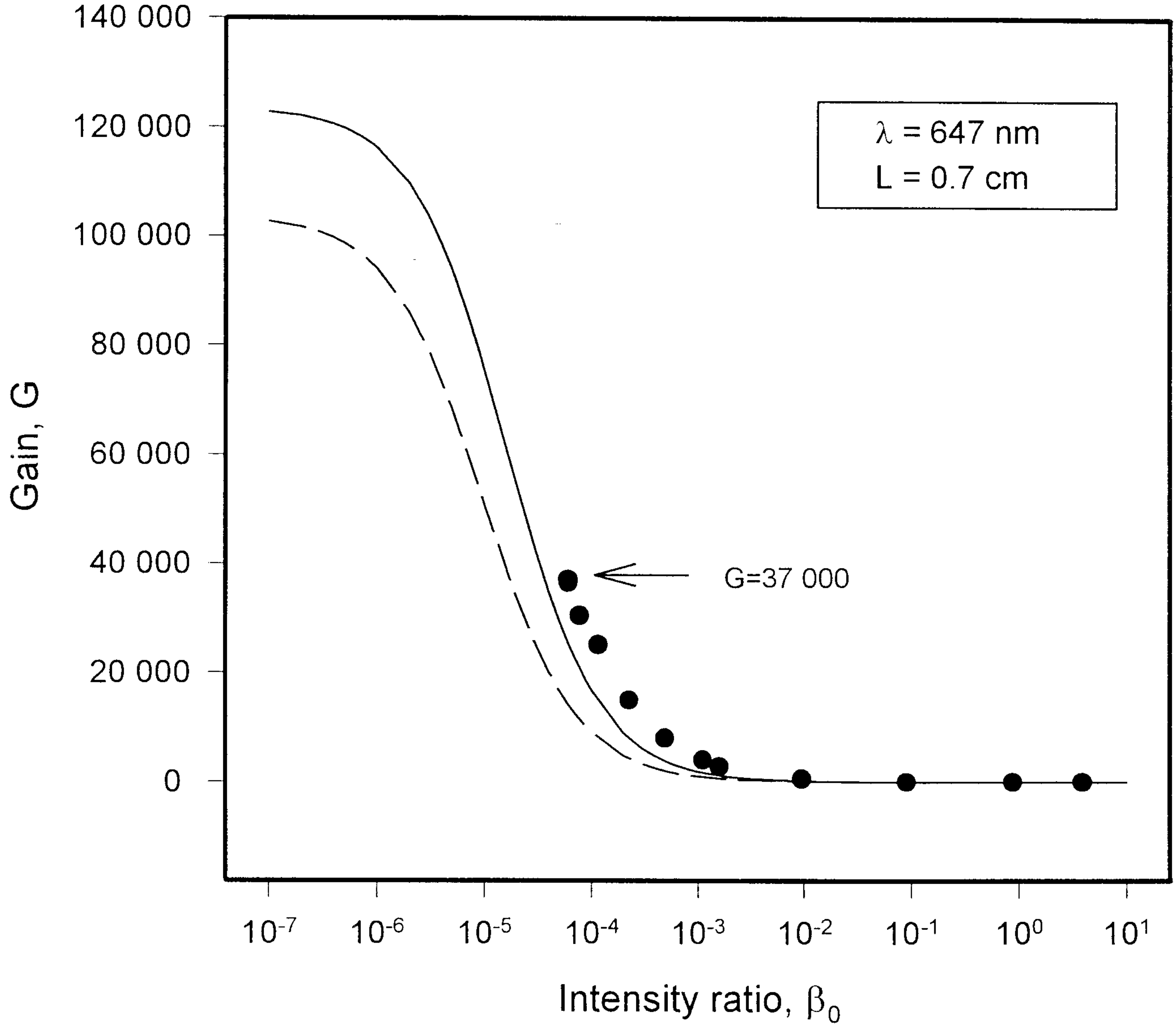

140 000
120 000
100 000
80 000
60 000
40 000
20 000
0
Gain, G
λ = 647 nm
L = 0.7 cm
G=37 000
10-7
10-6
10-5
10-4
10-3
10-2
10-1
100
101
Intensity ratio, β0

Fig. 2

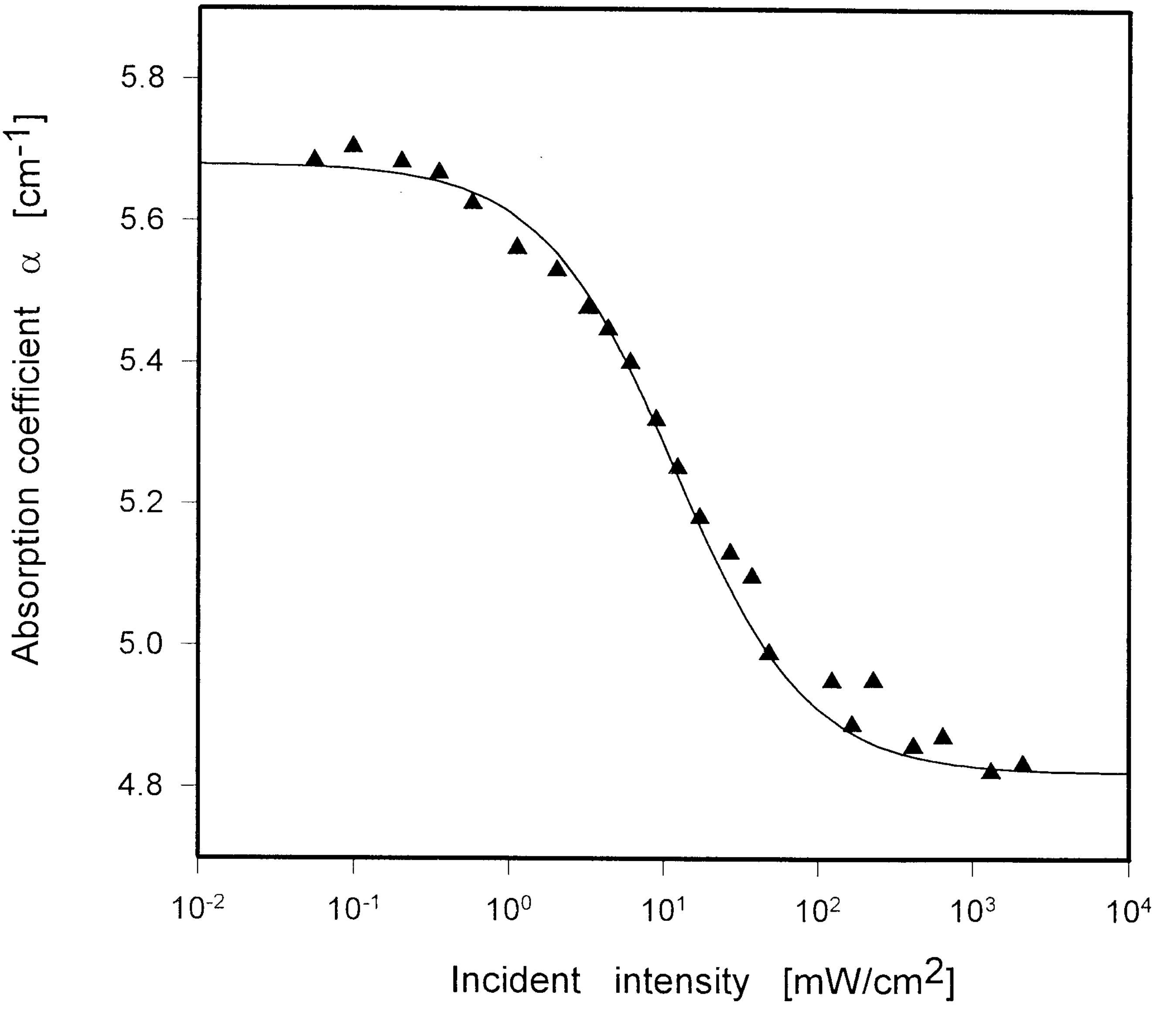
5.8
5.6
5.4
5.2
5.0
4.8
Absorption coefficient α [cm-1]
10-2
10-1
100
101
102
103
104
Incident intensity [mW/cm2]

Fig.3

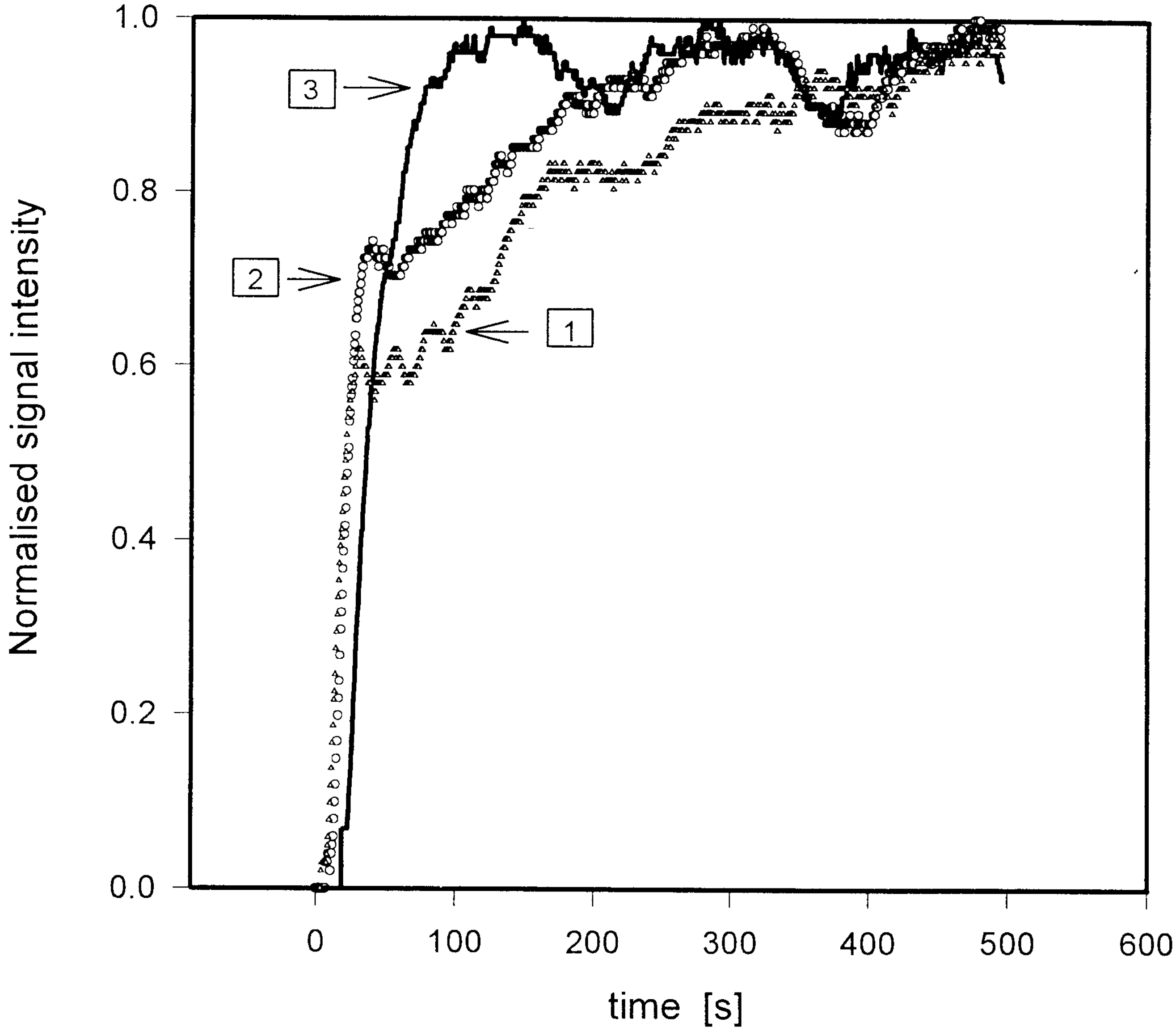

Normalised signal intensity
1.0
0.8
0.6
0.4
0.2
0.0
0
100
200
300
400
500
600
time [s]
3
2
1

Fig.4

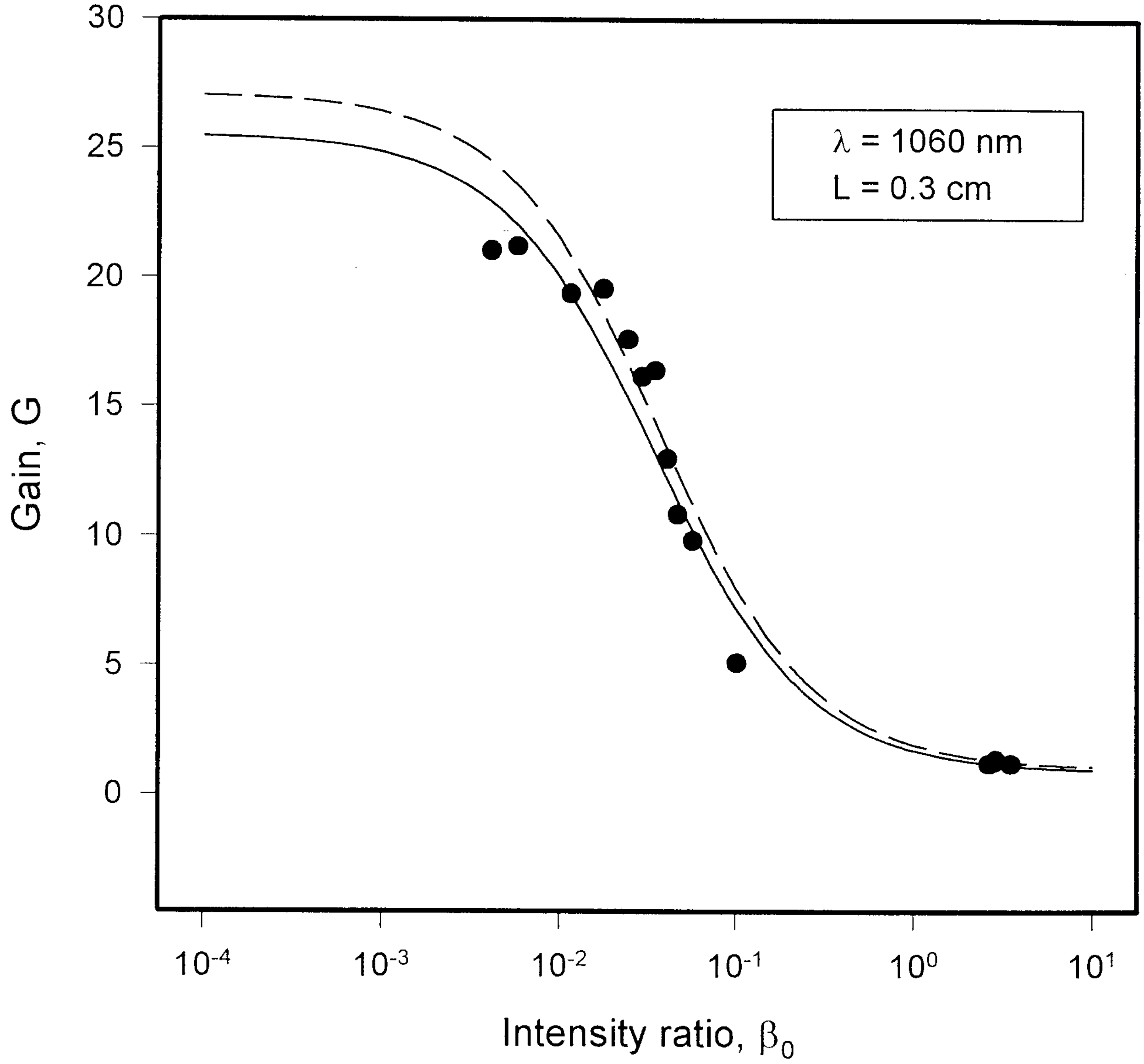

30
25
20
15
10
5
0
Gain, G
λ = 1060 nm
L = 0.3 cm
10-4
10-3
10-2
10-1
100
101
Intensity ratio, β0

Fig. 5